Available online at www.sciencedirect.com
SCIENCE DIRECT®
Journal of Organometallic Chemistry 685 (2003) 269–279
Journal of Organometallic Chemistry
www.elsevier.com/locate/jorganchem

Polysilylenes: charge carrier transport and photogeneration

Stanislav Nespurek [a,b,*], Julinz Sworakowski [c], Andrey Kadashchuk [d], Petr Toman [a]

[a] Institute of Macromolecular Chemistry, Academy of Sciences of the Czech Republic, Heyrovsky Sq. 2, 162 06 Prague, Czech Republic
[b] Faculty of Chemistry, Technical University of Brno, Purkynova 118, 612 00 Brno, Czech Republic
[c] Institute of Physical and Theoretical Chemistry, Wroclaw University of Technology, Wyb. Wyspianskiego 27, 50-370 Wroclaw, Poland
[d] Institute of Physics, National Academy of Sciences of Ukraine, Prospect Nauki 46, 03650 Kiev-39, Ukraine

Received 15 April 2003; accepted 26 April 2003

Abstract

Charge carrier transport and photogeneration in polysilylenes, specifically in poly[methyl(phenyl)silylene], are discussed. Electronic properties are influenced by electron delocalization along the silicon backbone. A model of disordered polarons seems to be adequate to describe the charge carrier transport properties. Dissociation of ion pairs in external electric field, which can be described in terms of the Onsager theory of geminate recombination, seems to be the main mechanism of the free charge carrier photogeneration. Polar additives or polar side groups attached to the polymer backbone locally modify the ionization energy of the polymer segments and energies of electrostatic interactions of charge carriers and the dipoles. These changes result in the creation of local states for charge carriers and in the formation of a potential well structure. If the side groups are photochromic species changing their dipole moments upon illumination, then a light-driven molecular switch can be proposed.
© 2003 Elsevier B.V. All rights reserved.

Keywords: Polysilylenes; Charge carrier transport; Photogeneration; Polaron; Molecular switch

1. Introduction

Polysilylenes (in literature also called polysilanes, polyorganosilanes, poly(organylsilanediyl)s, organopolysilanes, or catena-silicon polymers) are of considerable research interest because of their electronic, photoelectrical, and nonlinear optical properties, and the effect of σ-electron delocalization along the chain [1]. Optical and electrical properties of these polymers have been found to significantly differ from structurally analogous carbon-based σ-bound systems such as polystyrene and polyethylene, resembling rather fully π-conjugated systems like polyacetylenes. Physical properties are strongly influenced by the chemical structure of the polymer side groups; various polymers with photoconductive, electroluminescent, ionic, thermochromic, piezochromic, photorefractive, electro-optical, nonlinear optical, and liquid-crystalline properties can be synthesized [2,3]. Some of these properties could form a new basis for future electronics. For example, nonlinear optical properties, emission, and semiconductive properties are suggested to be useful for swift optical switches, light emission displays, photorefractive memories, and current molecular switches and modulators [4–6]. Several features, such as simple chemical synthesis and the possibility to obtain pure polymer by conventional techniques, easy processability due to good solubility, and optical transparency in the visible region, make polysilylenes suitable for applications.

In this paper, the charge carrier photogeneration and transport are discussed on a model material, poly[methyl(phenyl)silylene] (PMPSi), but some properties of other polysilylenes are also mentioned.

2. Experimental

In this chapter, we will briefly describe the chemical synthesis and methods, which were utilized for acquisition of the results mentioned below.

* Present address: Institute of Macromolecular Chemistry, Academy of Sciences of the Czech Republic, Heyrovsky Sq. 2, Prague 16206, Czech Republic. Tel.: +420-222-514-610; fax: +420-222-516-969.
E-mail address: nespurek@imc.cas.cz (S. Nespurek).

0022-328X/03/$ - see front matter © 2003 Elsevier B.V. All rights reserved.
doi:10.1016/S0022-328X(03)00648-X

2.1. Material

Currently, the best synthesis of high-molecular weight polysilylenes is the Wurtz coupling of dichlorosilanes [7]. However, this reaction has several drawbacks. The Wurtz coupling gives low yields (5–60%) and variable molecular weights. The harsh conditions of the synthesis exclude the incorporation of polar side groups into the monomer, and hence only a limited number of monomers can be used. An alternative and less hazardous method was discovered by Aitken et al. [8]. Titanium and zirconium metallocene complexes were found to perform dehydrogenative coupling of phenylsilane to form oligomeric poly(phenylsilylene). Its Si–H bonds undergo mild radical hydrosilylations with a wide variety of olefins and carbonyl compounds [9]. This synthesis opens the door to novel polysilylenes inaccessible by the Wurtz coupling method. All polysilylenes mentioned in this work were prepared by the methods described in Refs. [3,10].

2.2. Measurements

Measurements of "on-chain" charge carrier mobility were carried out using the time-resolved microwave photoconductivity (TRMP) [11]. Photocurrent measurements were performed by the time-of-flight (TOF) technique and charge carrier mobility was determined using the transit time [12]. The quantum generation efficiency was determined by the xerographic discharge method [13,14]. Photoinduced transient absorption was measured using the first harmonics (347 nm) generated with a ruby laser or the second harmonics (266 nm) generated with an Nd:YAG laser system [15]. Thermostimulated luminescence (TSL) measurements were performed in two different regimes: under uniform heating and in the fractional heating regime, which allows to determine trap depth [16].

3. Charge carrier transport

Polysilylenes consist of a chain of silicon atoms with interacting three sp^3 hybrid orbitals. The resonance integral between two sp^3 orbitals located on adjacent silicon atoms and pointing to each other, β_{vic}, is responsible for the formation of a Si–Si σ-bond (see Fig. 1). Electron delocalization along the silicon backbone results from the mutual interaction of sp^3 orbitals of adjacent silicon atoms [1]. The degree of electron delocalization in the backbone is a function of the β_{vic}/β_{gem} ratio, where β_{gem} is the resonance integral between two sp^3 orbitals localized on the same silicon atom. Electron delocalization is perfect if the ratio equals unity.

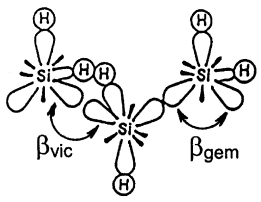

Fig. 1. The basis set of Si sp^3 and H 1s orbitals.

Thus, the linear Si backbone behaves as a molecular wire due to the σ-conjugation. The highest "on-chain" mobilities were detected as 2×10^{-5} m^2 V^{-1} s^{-1} [17]; the values in π-conjugated carbon polymers are usually higher (up to 7×10^{-5} m^2 V^{-1} s^{-1}). The mobilities of mobile charges (holes) depend on the chemical nature and on the size of the side groups. In alkyl-substituted polysilylenes, the hole mobilities seem to increase with increasing length of the alkyl substituent; for example, in poly[hexyl(phenyl)silylene] (PHPSi), the "on-chain" mobility equal to 2×10^{-5} m^2 V^{-1} s^{-1} was reported [17], whereas $\mu < 10^{-6}$ m^2 V^{-1} s^{-1} was found for poly[ethyl(phenyl)silylene] (PEPSi) by the time-resolved microwave conductivity technique [17]. The "on-chain" hole mobility in PMPSi was found to amount to $\mu \sim 2 \times 10^{-6}$ m^2 V^{-1} s^{-1} using TRMP [18].

Generally, three types of charged species can be detected by the microwave detection method: free and localized charge carriers, and correlated charges (i.e. dipoles). In organic semiconductors, in initial stages of the excitation, mainly electron–hole pairs, in which the separation between the charged species is smaller than the Onsager "escape distance", are detected. An initial part of a decay curve of the microwave signal then reflects the recombination kinetics of the pairs generated in the polymer main chain. The TRMP trace measured on PMPSi powder [18] is shown in Fig. 2. The signal shows a dispersive behavior: at least two components of the decay can be distinguished. The initial rapid decay of the microwave signal with a half-life $\tau_{1/2} = 80 \pm 20$ ns is followed by a slow process. The kinetics of the latter part of the signal can be fitted with a stretched exponential function up to the millisecond range.

Excitation at 355 nm in PMPSi results in the fast formation of electron–hole pairs in the Si backbone that undergo a fast chain geminate recombination to a

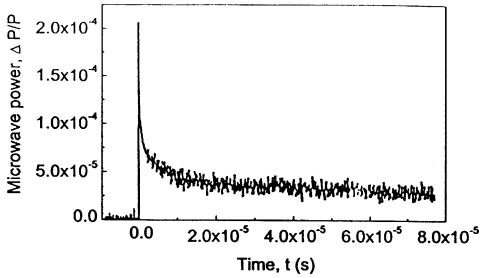

Fig. 2. TRMP trace for PMPSi: $\lambda_{exc} = 355$ nm; band with of the amplifier = 500 MHz.

significant extent. The remaining portion of ion pairs escapes the fast geminate recombination presumably due to the fact that σ-conjugation extents only over a limited number of silicon atoms with the consequence that only electron–hole pairs formed in the same conformational chain segment can recombine fast. The rest of electron–hole pairs relaxes to the ion pair (σ, π*) charge-transfer state. This implies a transfer of the electron from the silicon backbone to the pendant phenyl groups. This electron transfer is quite possible because the ground state is predominantly σ_{Si-Si}, i.e. ionization potential $I_p(Si-Si) < I_p(benzene)$ [19]. The photoelectron spectral band of benzene was found at 9.24 eV (π, e_{1g}) [20] and of hexamethyldisilane at 8.69 eV (σ_{Si-Si}) [21]. The Si–Si grouping is unique in the sense that I_p of the (σ_{Si-Si}) electrons is lower than that of the benzene π-electrons. The electron transfer to benzene ring is also in agreement with reduction experiments [22]. The case of reduction obeys the order $(Me_2Si)_5 > C_6H_6 > (Me_2Si)_6 > Me(Me_2Si)_nMe$, where Me is methyl.

For the homogeneous diffusion-controlled recombination of electrons and holes, the recombination half-time, τ_R, is given by the relation

$$\tau_R = \frac{\varepsilon\varepsilon_0}{e\mu N} \quad (1)$$

where $\varepsilon\varepsilon_0$ is the electric permittivity, e the unit charge, μ the charge mobility, and N the pair concentration. Taking τ_R ($=\tau_{1/2}$) from the fast part of the experimental kinetics (N was determined by calibration of the microwave signal using TiO_2), one can estimate the value of the on-chain mobility as 2×10^{-6} m^2 V^{-1} s^{-1} in a good agreement with the data presented in Ref. [23]. This value is very probably still limited by conformational disorder and structure defects in the backbone. In the case of the polysilylene chain, a perfect all-trans arrangement of the σ-bonds has been shown to be the optimum configuration of intrachain electronic coupling [1,24]. Lower "on-chain" mobilities in σ-conjugated polymers in comparison with π-conjugated polymers can be attributed to a greater conformational disorder and a decrease in the overall electronic coupling due to lower barriers to conformations other than all-trans. The longtime decay process can be related to the intrachain recombination (Si chain cation radicals with phenyl anion radicals) and/or to the interchain electron–hole recombination. The latter value must be close to the zero-field drift mobility measured on 3D samples as was indeed observed (at room temperature $\mu(F \to 0) \approx 10^{-9}$ m^2 V^{-1} s^{-1} [14]; from the measurements of microwave conductivity, 2×10^{-9} m^2 V^{-1} s^{-1} was obtained [23]).

A question arises why the values of "on-chain" mobilities are so low. A possible reason is the formation of polarons. The strong electron–phonon coupling causes carrier self-trapping and creates a quasiparticle, a polaron, which can move only by carrying along the associated molecular deformation. The motion of such a charge carrier, dressed into a cloud of local deformation of the nuclear subsystem, can be phenomenologically described by introducing a temperature-dependent effective mass which is higher than the electron mass. A significant distortion of the PMPSi chain was recently found by Kim et al. [25] by measuring the migration rate of the excitation energy along the polymer chain. The results of quantum chemical calculations shown in Fig. 3 demonstrate that the presence of the charge in the molecule indeed deforms the chain [11].

Another important feature influencing the charge movement on the polymer chain is the presence of traps. An isolated macromolecule is a 1D system in which the presence of any defect results in a localization of charge carriers [26]. Let us consider a system containing traps, which are neutral when empty. In a 3D system, once such traps are filled, they act as scattering centers for other carriers approaching their sites, without otherwise hindering their motion. The situation is, however, qualitatively different in 1D systems. Any localized carrier becomes an obstacle rendering it impossible for another carrier to follow the same path. Because in strictly 1D systems the probability of lateral jumps is zero, any filled "primary" trap produces a "secondary" localization center at a distance of the order of the coulombic radius. In other words, a single primary trap may localize several carriers. This phenomenon was referred to as "degenerate trapping" [27].

It is not simple to experimentally detect the polaron formation. One possibility is using the technique of TSL [28]. The method is based on the fact that TSL

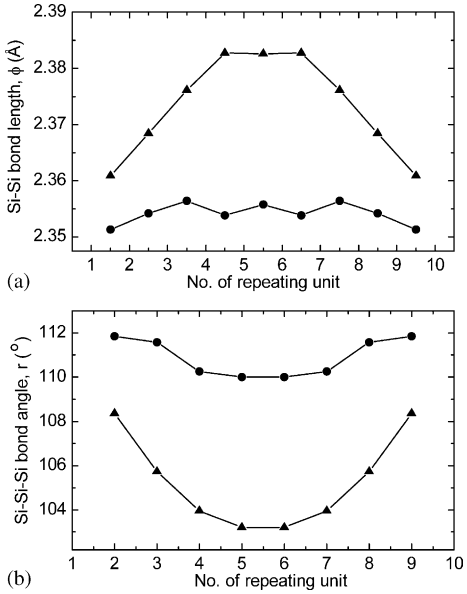

Fig. 3. Changes of Si–Si bond lengths (a) and Si–Si–Si bond angles (b) during the positive polaron formation (▲) in deca[methyl(phenyl)silylene]. Symbols (●) are for defect-free case.

measurements are performed after some dwell time on samples, which have been photoexcited at liquid helium temperature, and the initial distribution of polarons is formed in the course of low-temperature energy relaxation. Polaron formation strongly affects both low-temperature energy relaxation and thermally assisted hopping of charge carriers in disordered material. If the polaron binding energy is comparable with or larger than the density-of-states (DOS) width, the energetically downward hopping is strongly suppressed by the lack of deeper vacant sites, which are only accessible for further jumps at low temperatures. Therefore, after a fast initial polaronic relaxation, the energy distribution of polarons remains almost "frozen in" over the entire dwell time between low-temperature photoexcitation of the sample and the onset of the TSL heating run. With increasing temperature, energetically upward polaron jumps become the dominant hopping mode and these jumps control the TSL kinetics. The polaronic contribution to the activation energy of every individual upward jump is equal to half of the polaron binding energy, $E_p/2$, while the low-temperature energy relaxation of polarons within the DOS distribution is slowed down because the polaron energy distribution is shifted down by E_p. This leads to a stronger polaronic effect on the low-temperature relaxation than on the thermally stimulated hopping. Therefore, at moderate values of E_p, the polaronic effect shifts the TSL peak to lower temperatures as compared with its position for a material with a similar DOS width and with $E_p = 0$.

The polaron occurrence can be treated by additional infrared (IR) irradiation after photoexcitation and before the TSL run measurement. IR irradiation causes local heating in the environment of charged molecules and at low temperatures efficiently stimulates energy relaxation towards the deeper tail states of polarons. Concomitantly, charge carriers get a possibility to occupy those tail states, which would be accessible for them when there were no polaron effects. This results in the shift of the TSL peak towards higher temperatures and in a decrease in its intensity. Experimental data for PMPSi and poly[biphenyl-4-yl(methyl)silylene] (PBMSi) are given in Fig. 4 [28]. The polaron binding energy in PBMSi is higher because of the stronger charge coupling to the torsional mode of the biphenyl unit and, therefore, we observe a larger shift of the TSL curve maximum after IR irradiation.

Fig. 5 illustrates the dependences of the charge carrier mobility, μ, of a 3D PMPSi sandwich sample (thickness ca. 2 μm) on F, the electric field strength, at different temperatures. In all cases, the mobility can be described by an $\exp(\beta F^{1/2})$ dependence for $F > 10^7$ V m^{-1}. At lower field strengths, $\mu(F)$ becomes constant or increases slightly upon reducing F. This behavior [12] is in agreement with the data published by Bässler et al. [29], but at variance with the data of Abkowitz and Stolka

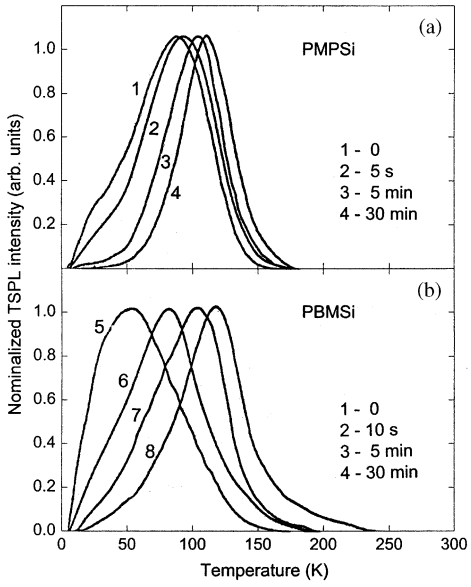

Fig. 4. Normalized TSL glow curves of (a) PMPSi and (b) PBMSi measured after UV excitation at 4.2 K (curves 1 and 5) and after additional IR irradiation (curves 2–4 and 6–8).

[30] who reported a ln μ vs. $\beta F^{1/2}$ dependence extending over two decades to $F = 10^6$ V m^{-1}. These types of dependences are usually treated in the framework of the hopping disorder concept. The essential difference between the polaron and disorder models is that the latter, at variance with the former, implies a sufficiently weak electron–phonon coupling and the activation energy of charge transport reflects the static energy disorder of the hopping sites. In contrast, the polaron model suggests a strong electron–phonon coupling and

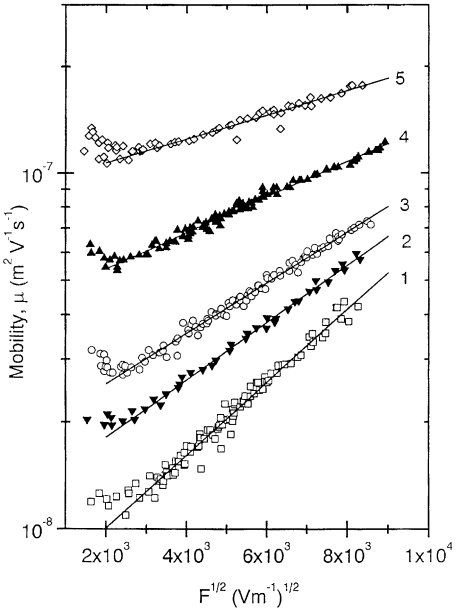

Fig. 5. Electric field dependence of the mobility of PMPSi parametric in temperature: $T = 295$ K (curve 1), 312 K (curve 2), 325 K (curve 3), 355 K (curve 4), and 358 K (curve 5).

a negligible contribution of energy disorder to the activation energy of the carrier mobility. Since the structural distortion is an intramolecular process, polaron binding energy E_p is not subjected to meaningful variation. Concomitantly, the polaronic charge transport must obey the Gaussian statistics and the photocurrent transients should neither feature a long tail nor become dispersive at any temperature. However, these predictions were not confirmed experimentally in polymers. In addition, the small polaron model fails to account for the observed Poole-Frenkel-type field and non-Arrhenius temperature dependences of the thermal equilibrium carrier mobility. It was suggested [14,29,31] that the zero-field activation energy of the mobility, $E_a^*(F \to 0)$, can be approximated by the sum of the disorder and polaron contribution as

$$E_a^*(F \to 0) = E_a^{pol} + E_a^{dis} = \frac{E_p}{2} + \frac{4}{9}\frac{\sigma^2}{(kT)^2} \quad (2)$$

where E_a^{pol} and E_a^{dis} are the polaronic and disorder contributions, respectively, σ the energy width of the DOS distribution, k the Boltzmann constant, and T the temperature. Usually it is difficult to distinguish from experimental data between $\mu(1/T^2)$ and $\mu(1/T)$ dependences. Then, the second term of Eq. (2) can be treated as an apparent (effective) activation energy which can be expressed as $E_a^{eff} = E_p/2 + (8/9)\ \sigma^2/kT$.

The polaron binding energy was determined for PMPSi [29] as $E_p = 0.16$ eV, for PBMSi as $E_p = 0.22$ eV [12]. Recently, Pan et al. [32] reported a smaller value of $E_p = 0.08$ eV for PMPSi. The E_p values are still an open question and need more measurements and discussions. For PMPSi, the zero-field value of the activation energy of the mobility was measured as $E_a^*(F \to 0) = 0.29$ eV. The effective value of the half-width of the Gaussian distribution of the hopping states σ^* was determined from the equation $E_a^*(F \to 0) = (8/9)(\sigma^{*2}/kT)$ as 0.093 eV (at room temperature). From TSL studies, the value $\sigma^* = 0.096$ eV was obtained in good agreement with the transport data. The real value of the width of the distribution of hopping sites σ would be lowered by the polaron contribution $(E_a^* - (E_p/2) = 8\sigma^2/9kT)$; this yields $\sigma = 0.078$ eV.

It is interesting to try to change the transport parameters by doping [12]. The dopands can be divided into two groups: (i) materials with high electron affinity and zero dipole moment, like 7,7,8,8-tetracyano-1,4-quinodimethane (TCNQ), 2,3,5,6-tetrabromo-1,4-benzoquinone (BR), 2,3,5,6-tetrachloro-1,4-benzoquinone (CHL), and tetracene (TC), increase charge carrier mobility and decrease the σ^* parameter [12]. The mobility increases with increasing electron affinity of the acceptor. At the moment it is not clear what is responsible for this effect, the decrease in the polaron binding energy or disorder parameter σ; (ii) dopands with high dipole moments, like *o*-dinitrobenzene (DNB) or 1-benzamido-4-nitronaphthalene (BANP), decrease the charge carrier mobility, while the effective σ^* parameter increases. The detailed analysis shows that in this case charge–dipole interactions are important. Two effects must be mentioned in this context: (1) a broadening of the energy distribution of hopping states [12,33–35]; the mobility depends on the dipole moment (decreases with increasing dipole moment), the molecular dimensions of the additive, and the additive concentration. (2) New local states are formed in the vicinity of dipolar species [36–38] even though these molecules do not necessarily have to act as trapping sites. It should be indicated that the polar species should form traps for both electrons and holes. However, contrary to the situation encountered in the case of both the chemical traps and the "conventional" structural traps, the electron and hole traps are formed in different molecules: a molecule close to the negative pole of the dipole should be a hole trap, whereas a molecule close to the positive pole should trap electrons. If the guest molecule is located in the vicinity of a structure defect, such a feature of dipolar traps may lead to an asymmetry of trapping parameters for electrons and holes.

4. Electronic structure

Polysilylene chains, with two organic groups on each silicon atom, behave as 1D systems with weak intermolecular interactions. Molecular features of the material are reflected in the energy diagram of electronic states. As follows from Fig. 6, three bands were detected in UV absorption spectra [39] of PMPSi. The dielectric function provides a reasonable fit of the reflectance throughout the whole measurement range. While the three high-energy bands are single broad Gauss–Lorentz profiles, the lowest energy band seems to be represented by the cluster of several components. The

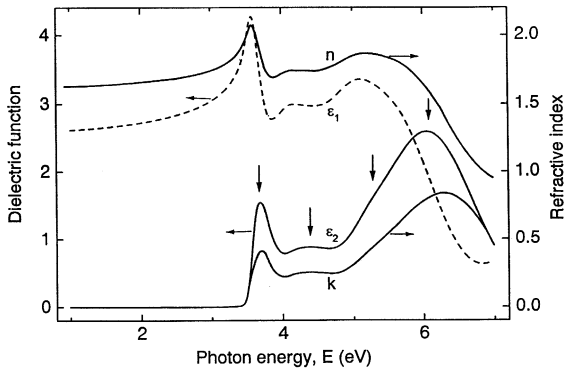

Fig. 6. Real (dashed line) and imaginary (solid line) parts of complex dielectric function and complex refractive index.

complex refractive index, $n+ik=\sqrt{\varepsilon}$, computed from the dielectric function is also given in Fig. 6. It has been shown [40] that the first longest wavelength absorption band ($\lambda_{max}=338$ nm for solid PMPSi films) is mainly due to delocalized σ–σ* transitions. The energy of these transitions is conformation-dependent and also depends strongly on the length of the molecule. The contribution of π–π* transitions to the longest wavelength band is weak in PMPSi. In polymers with polynuclear aryl substituents (e.g. naphthyl, biphenylyl), this absorption is better characterized as a localized π–π* excitation with a participation of a weaker σ–σ* one. The π–π* aryl-like excitations in PMPSi are responsible for the shorter-wavelength absorption (maximum at about 276 nm for solid PMPSi). Using a $(h\nu \times \alpha_0)^2$ vs. $h\nu$ plot (α_0 is the absorption coefficient), the band gap energy of PMPSi was estimated as $E_g=3.5$ eV. The band theory calculations [41,42] have suggested that the first strongly allowed optical transitions at 3.5–4.0 eV (calculated) result from band-to-band transitions in PMPSi. The lowering of E_g in comparison with the value of 4.5 eV for poly(dialkylsilylene)s was ascribed to a (σ, π) band mixing at the valence band edge state [43] between the skeleton Si 3p and π HOMO states of benzene rings as side chain substituents.

The energy diagram is schematically given in Fig. 7. At least three subbands associated with polymer branching (E_{BP}), defect states formed by the backbone scission E_t^h ($E_v - E_t^h \sim 0.45$ eV) [16], and the charge-transfer $^1(\sigma, \pi^*)^{CT}$ state were detected at low temperatures. In electroabsorbance measurements of PMPSi [44] at 4.68 eV, a peak was found. This is evidently not the result of a Stark shift of a normal absorption band but it arises from electronic transitions that result in a large change of polarizability and could be associated with charge transfer among polymer segments or chains.

As it follows from the fluorescence emission measurements, the photoluminescence (PL) of PMPSi (transition (i) in Fig. 7) consists of a relatively sharp band with the maximum at 357 nm and a significantly broad emission in the visible part of the spectrum. The sharp emission is associated with the σ*–σ deexcitation. A remarkable feature of the behavior of broad visible luminescence is that its maximum at 5 K is situated at about 415 nm, while at $T>100$ K, the maximum is shifted to about 500 nm [45]. The last mentioned luminescence is, at least partly, associated with the transitions from luminescent branching points E_{BP} (transition (ii) in Fig. 7). The important property of the visible luminescence is that it is stronger when the excitation is carried out by π–π* transitions of the phenyl substituent in PMPSi as compared with the σ–σ* excitation of the silicon skeleton. This could be associated with the fast beginning geminate recombination of charges generated during the σ–σ* excitation. The subsequent electron transfer to phenyl group forms a charge-transfer (CT) exciton [46]. On the basis of the detailed analysis of aryldisilanes and related compounds [46], it was stated that the fluorescence from the intramolecular charge-transfer state $^1(\sigma, \pi^*)^{CT}$ is located at about 400 nm. Thus, we can assume that the short-wavelength visible luminescence at about 415 nm is associated with the emission from the $^1(\sigma, \pi^*)^{CT}$ charge-transfer state (transition (iii) in Fig. 7). It is interesting to

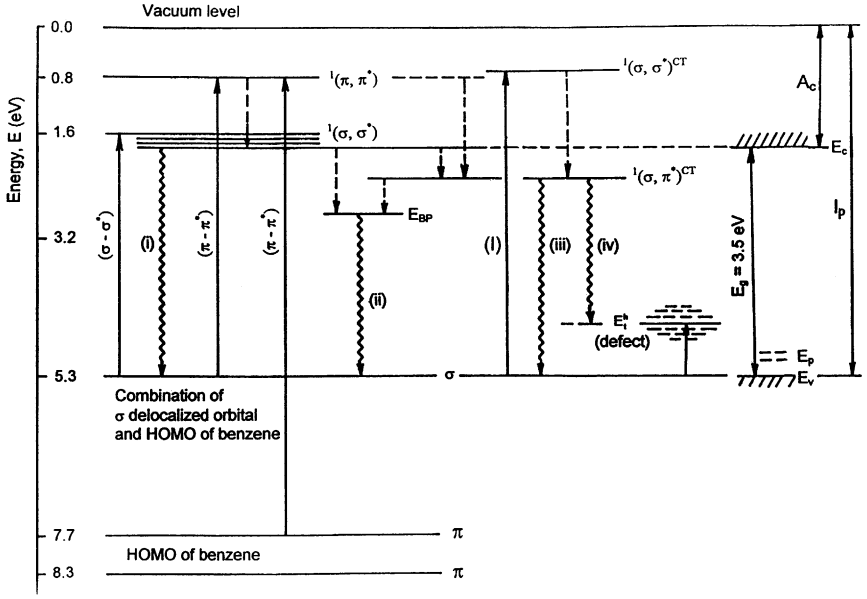

Fig. 7. Schematic energy diagram of PMPSi. E_{BP} is the energy of branching points, E_t^h the defect (Si–Si bond scission) level, E_p the polaron level, E_v and E_c the energies of the edges of the valence and conduction bands, respectively, E_g the energy gap, and $^1(\sigma, \pi^*)^{CT}$ and $^1(\sigma, \sigma^*)^{CT}$ the energies of intramolecular and intermolecular charge-transfer states, respectively. σ–σ* and π–π* represent the electronic transitions due to the light excitations.

test the charge-transfer luminescence during the formation of defect states, i.e. during the chain photodegradation ($\lambda_{irr} = 365$ nm at room temperature). It is known that the chain scission forms the trapping states (cf. E_t^h level in Fig. 7) [16,47] for holes. Then, in addition to the emission at 410 nm, a new band in the spectral region 520–540 nm was observed. Visually, the color of the PL changed from blue for a virgin sample to light-green for the photodegraded sample. This effect could be associated with interactions of intramolecular CT excitons with holes localized at traps 0.45 eV (cf. E_t^h level) deep (cf. transition (iv) in Fig. 7). It follows from our previous studies [16] that the trapping states are metastable and can be annealed thermally. The transformation of PL from blue to light-green follows the trap formation, whereas the transformation of PL from light-green back to blue follows the trap annealing (measured at low temperatures). Thus, the blue PL can be reversibly switched to the light-green PL by UV irradiation at room temperature and back from light-green to blue PL by thermal annealing. It should be pointed out that the blue PL recovery can also be stimulated by the 255 nm light. This unexpected behavior can be explained by photoexcitation of trapped electrons localized in the benzene rings.

5. Charge carrier photogeneration

Optical excitations in polysilylenes lead to the charge carrier photogeneration. If polymer (we will discuss here an example of PMPSi) is excited by light of energy $E >$ 4.7 eV, the charge-transfer state $^1(\sigma, \sigma^*)^{CT}$ is formed (see Fig. 7) and a direct electron transfer among macromolecules is possible. In the external electric field a photocurrent can be detected [48]. In the case of σ–σ^* and π–π^* electronic excitations, somewhat more complicated mechanism must be taken into account. Both the excitations lead to the formation of the $^1(\sigma, \pi^*)^{CT}$ charge-transfer state (bound ion pairs). The electron in the phenyl radical anion is localized, whereas hole in the radical cation state is delocalized over the silicon main chain. Under the influence of an external electric field, the ion pairs can dissociate and free charge carriers can be formed. The electric field dependences of the photogeneration efficiency, η, as taken by the electrophotographic discharge method are shown in Fig. 8 for light of $\lambda_{inc} = 254$ and 355 nm incident upon a positively charged surface [49]. The full lines are the best fits using the Onsager theory of geminate recombination modified by the Gaussian distribution function of ion pair radii [50]. The fitted parameters yielded primary quantum efficiency η_0 (the number of ion pairs created by one photon) and separation distance r_0; for 254 nm illumination $\eta_0 = 0.9$ and r_0 ranged from 1.5 to 3.0 nm (at high and low applied electric fields), for 355 nm illumination

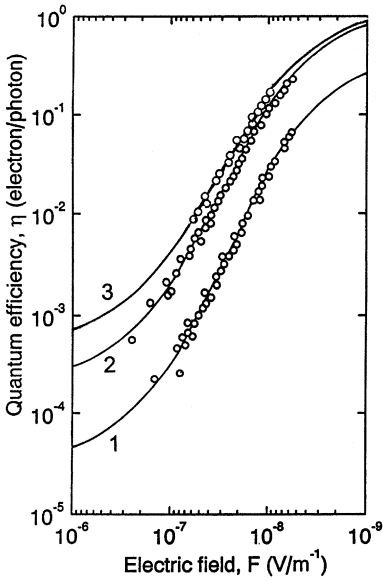

Fig. 8. Electric field dependences of the photogeneration efficiency ($T = 300$ K) in PMPSi at $\lambda_{exc} = 355$ nm (curve 1) and 254 nm (curve 2), and in copolymer (PMPSi–DNPH, curve 3) at $\lambda_{exc} = 355$ nm. Full lines are the best fits using the Onsager theory of geminate recombination with the distribution of radii of ion pairs. Taken from Ref. [49]. Curve 3 represents the dependence for PMPSi–DNPH copolymer (at $\lambda_{inc} = 355$ nm).

$\eta_0 = 0.45$ and r_0 ranged from 1.3 to 2.6 nm. The ion pairs with shorter separation distances can participate in the dissociation step only at higher electric fields; these pairs usually strongly recombine at low fields.

If some acceptor groups are chemically attached to the polymer (e.g. copolymer PMPSi–DNPH; Scheme 1), the separation distances are larger (see curve 3 in Fig. 8) and the photogeneration efficiency is higher. The geminate recombination is limited. The separation distances for copolymer PMPSi–DNPH were found to range from 1.6 to 3.2 nm (high and low electric field values, respectively). The primary quantum generation efficiency of ion pair formation was found to be twice higher for PMPSi–DNPH than for PMPSi ($\lambda_{exc} = 355$ nm) [51]; at a low field, the photogeneration efficiency was more than one order of magnitude higher. Electron acceptors make the electron transfer and the process of formation of ion pairs more effective. Similar results were obtained by acceptor doping [12].

It could be pointed out that some published quantum efficiency vs. electric field dependences obtained by the laser flash method on sandwich-type samples ITO/PMPSi/Al [48,52] differ from the Onsager curves. Laser flash measurements using different electrode materials showed that in these types of samples the electric field dependences of the apparent quantum efficiency η can be analyzed in the frame of electrode-limited photoinjection [53]. For the samples irradiated through ITO electrode, the dependence followed the relation $\eta = \eta_0 \exp(-bF^{-1/2})$, where η_0 and b are constants. For

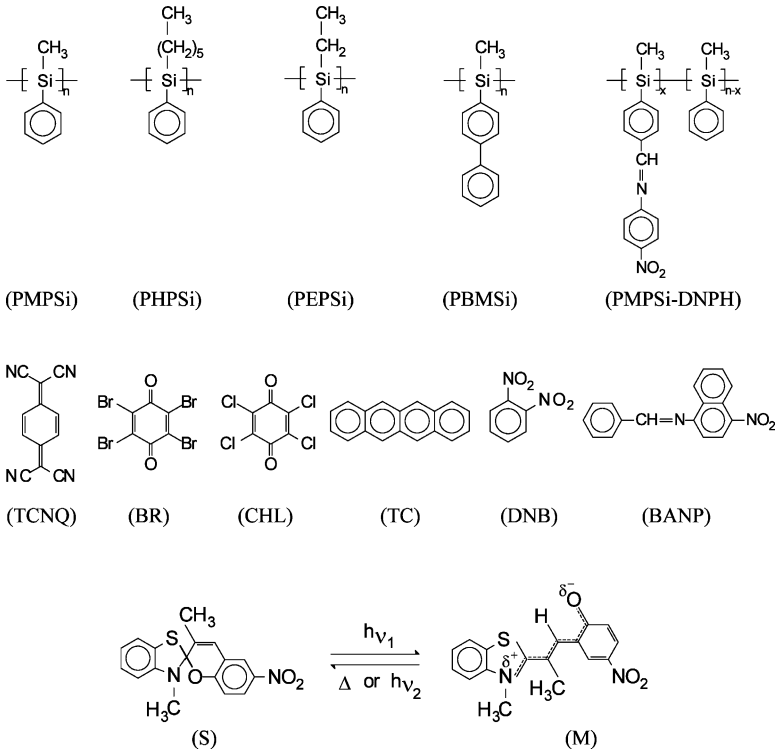

Scheme 1. Chemical structures of materials mentioned in this paper.

the irradiation through the gold electrode, the electrode-limited photoinjection was not so strong and at higher electric fields Schottky emission prevailed; the electric field dependence of the photogeneration efficiency could be fitted by the relation $\eta = \eta_0 \exp(aF^{1/2} - bF^{-1/2})$, where a and b are constants. Thus, the contactless electrographic discharge method is the best way to get a true dependence of the photogeneration efficiency on electric field.

To get more information about the formation of ion species during the excitation, the flash photolysis experiments were performed. Fig. 9 shows transient optical absorption spectra of PMPSi in tetrahydrofuran solution which were obtained during the 20 ns flash of the 347 nm light. The spectrum shows a rather strong maximum at 380 nm and two weaker maxima at about

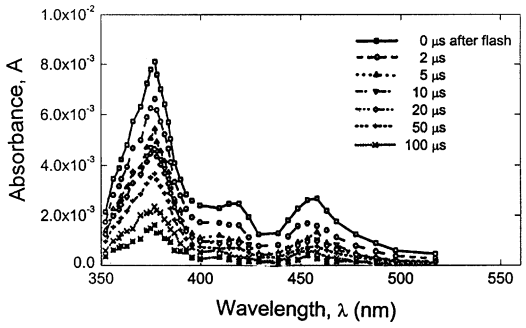

Fig. 9. Flash photolysis spectra of PMPSi in Ar-saturated tetrahydrofuran solution ($\lambda_{exc} = 347$ nm).

420 and 460 nm. The absorbance in the main maximum was determined as 0.009. The spectrum in the solid state shows a similar character.

The peak at 380 nm is ascribed to absorption of poly(silylene) radical cation according to literature data [54,55]. The half-time of the radical cation can be estimated from decay curves as about 50 μs for PMPSi in solution, and about 20 μs for PMPSi in the solid state. The weaker absorption in the spectral region 400–500 nm could be attributed to silyl radical $^{\bullet}SiR_2$ [56], partly to silylene biradicals $:SiR_2$ [57]. Phenyl anion radicals could not be detected in our experiments because it absorbs mainly at 260 nm [58]. During the photoexcitation of Si skeleton electrons, the bonding electron is transferred into the non-bonding state and a cation radical is formed. The process is also accompanied by the formation of weak Si–Si bonds and bond scission. In the oxygen atmosphere very often siloxane structures are formed, and in oxygen-free atmosphere the process of the formation of weak Si–Si bonds and hole traps is reversible. If the electrical conductivity detection method [14,15,51] was used simultaneously with the technique of optical transient absorption, a photocurrent was detected. Kinetic measurements of the decay of both optical absorption and photocurrent after the flash revealed in all cases a correlation between the decay rates of the absorbance at 380 nm and the photocurrent, thus substantiating that the ionic species detected by changes in the electrical conductivity are light-absorbing at this wavelength. The determined quantum yield of the

radical cation formation, $\eta(\text{ion}) = 1 \times 10^{-2}$ ion per photon (for PMPSi/THF), is much higher than rate constants of diffusion-controlled reactions which might indicate a strong delocalization of ionic sites in the polymer backbone.

6. Polysilylene-based molecular devices

Quite efficient charge carrier transport properties of polysilylenes and possible modulation of the charge carrier mobility by charge–dipole interactions give a possibility to design a molecular electronic element, light-driven molecular switch [6,11]. The switch consists of a σ-conjugated molecular wire with photochromic side units chemically attached via a spacer [6,36]. There are many photochromic materials which can be used for this purpose (see, for example, Ref. [59] and references therein); here, we mention 6-nitro-1′,3′,3′-trimethylspiro[2H-chromene-2,2′-indoline] (see Scheme 1 (S–M)). The dipole moment of the stable form of a spiro molecule (S) amounts typically to 2–7 D depending on substituents attached to its skeleton; the dipole moment of the respective metastable form (merocyanine, M) may exceed 15 D. The overall mechanism can be described as a heterocyclic bond cleavage and ring opening, but there are also *cis–trans* transition and triplet–triplet contribution to the mechanism.

There are two limiting factors for the chemical structure of the spacer. The spacer can be "quasi-neutral" from the point of view of the charge transfer or it can freely transfer the charge during the formation of the dipole in the side group. In the former case, the electrostatic contribution of the polar side groups, based on the charge–dipole interactions, is the most important factor influencing the behavior of the charges on the molecular wire and can lead to the formation of a quantum-wall structure (see Fig. 10) [35]. In the latter case, the situation is more complex: the change of the chemical structure and a charge redistribution on the substituent, and a charge redistribution between the molecular wire and the photochromic group during the photochemical transformation may influence the ionization energy of the entire polymer segment containing the polar side group. Such a modification may result in the formation of a chemical charge carrier trap on the segment [60]. The formation of local states for holes during the photochromic transformation can also be inferred from the character of the orbitals as follows from Fig. 10 [11]. The character of the HOMO "S" orbital of PMPSi-S (PMPSi with spiropyran side group) Fig. 11 is nearly the same as that of PMPSi; a higher energy (cf. the energy scale in Fig. 7) orbital HOMO-1 "S" localized. During the phototransformation the orbital HOMO "M" maintains nearly the same energy level, as HOMO "S" but orbital HOMO-1 "S" is shifted to a lower energy and represents actually a localized HOMO-LOC "M" level. Thus, after the phototransformation, the charge is localized on the M side group. To be re-activated to the main chain, this charge should overcome the potential barrier [E(HOMO-Si) − E(HOMO-LOC "M")] ~ 0.5 eV and move through the backbone. Alternatively, it can tunnel between the side groups of the molecular wire provided the intersite distances are sufficiently short.

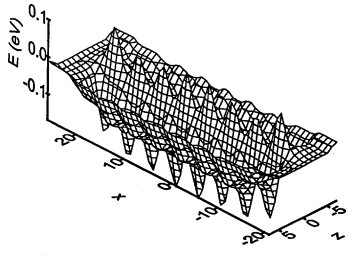

Fig. 10. Changes of local values of the polarization energy in the model system due to the presence of an array of eight parallel dipoles, 4D each. The array extends along the x-axis and the dipoles are parallel to z-axis. The distances between neighboring dipoles mimic the situation in PMPSi–DNPH copolymer containing 20% polar groups.

7. Conclusion

Electronic transitions of polysilylenes are influenced by one-dimensionality of the chain and weak intermolecular interactions. The energy gap is determined by HOMO and LUMO levels, giving the value 3.5 eV for PMPSi. In addition to $^1(\sigma, \sigma^*)$ (main chain) and $^1(\pi, \pi^*)$ (side groups) excited states, the charge-transfer $^1(\sigma, \pi^*)^{CT}$ state plays an important role in the photoconductivity and luminescence.

The charge carrier photogeneration is a multistage process which includes:

i) σ–σ* excitations of the Si backbone and/or π–π* excitation of the π-conjugated side groups and formation of $^1(\sigma, \pi^*)^{CT}$ charge-transfer state.
ii) The relaxation of the charge-transfer state and polaron pair formation.
iii) The dissociation of the polaron pair into free charge carriers in an external electric field.

The charge carrier (hole) transport proceeds predominantly along the σ-delocalized Si backbone with participation of interchain hopping and polaron formation. A model of disordered polarons seems to be adequate to describe the charge carrier transport properties. The intragap level of the hole polaron actually represents the pertinent "transport state".

Good solubility and ability to form thin films of good optical quality, optical nonlinearity, efficient lumines-

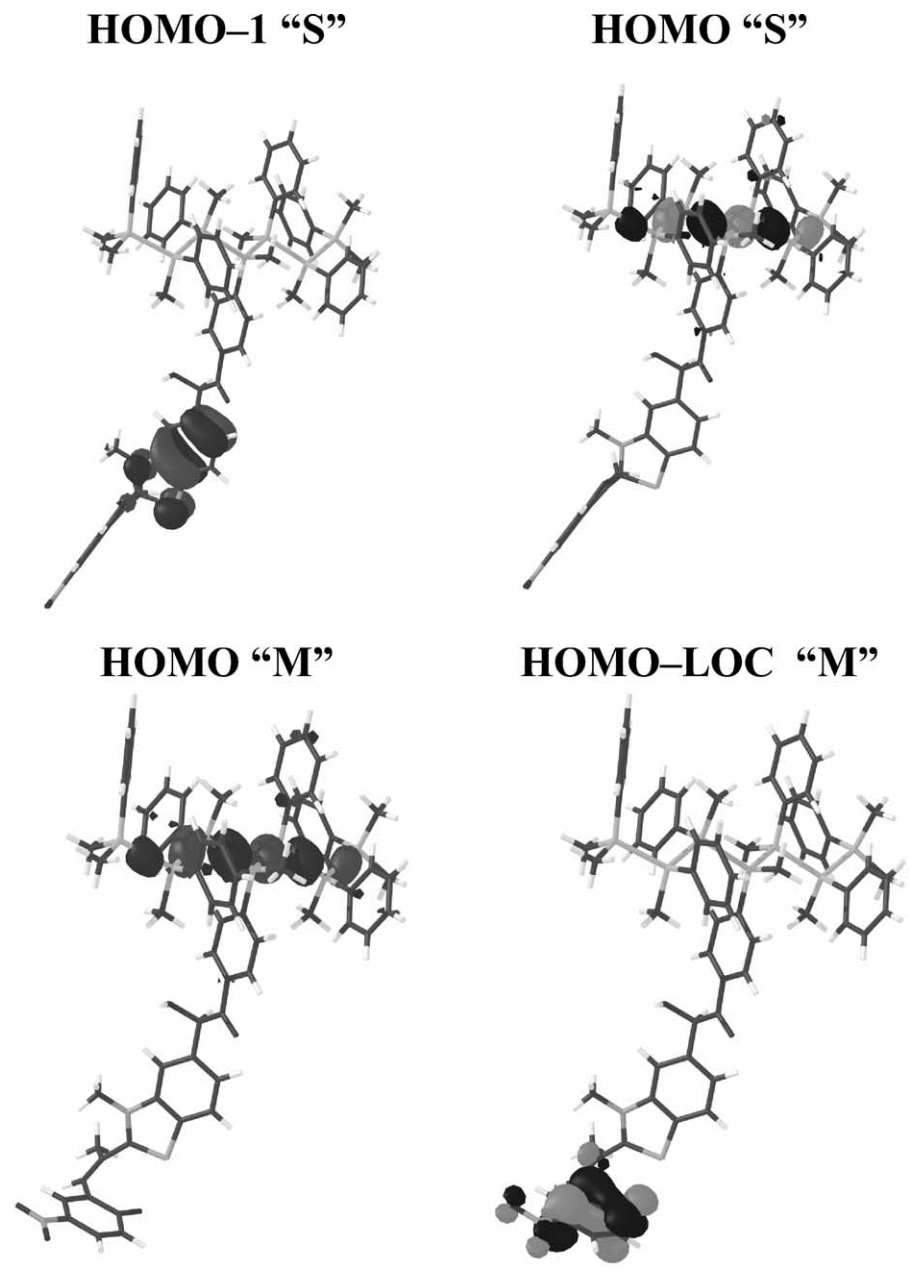

Fig. 11. HOMO orbitals of the PMPSi molecular wire with spiropyran side groups in closed S and open M form. HOMO-LOC "M" means the orbital where charge is localized after the phototransformation.

cence, high charge carrier photogeneration efficiency, and mobility suggest that this group of polymers could be used for optoelectronic applications in the future. Good transport properties allow to use the polysilylene skeleton as molecular wire in molecular electronic devices.

Acknowledgements

The work was sponsored by the Grant Agency of the Czech Republic (Grant No. 202/01/0518). This review article was written on the basis of many experimental and theoretical studies. The author would like to express his thanks for successful cooperation, namely to Dr. V. Cimrová (photoconductivity measurements), Dr. A. Eckhardt (TOF and flash photolysis measurements), Dr. I. Kmínek (chemical synthesis), Dr. H. Valerián (calculation of electron–dipole interactions), Prof. W. Schnabel (useful discussions), and Profs. V.I. Arkhipov and I.I. Fishchuk (polaron formation).

References

[1] R.D. Miller, J. Michl, Chem. Rev. 89 (1989) 1359.

[2] S. Chayase, Chemtech 24 (1994) 19.
[3] I. Kmínek, S. Nešpůrek, E. Brynda, J. Pfleger, V. Cimrová, W. Schnabel, Collect. Czech Chem. Commun. 58 (1993) 2337.
[4] R. West, J. Organomet. Chem. 300 (1986) 327.
[5] I. Bleyl, K. Ebata, S. Hoshino, K. Furukawa, H. Suzuki, Synth. Met. 105 (1999) 17.
[6] S. Nešpůrek, J. Sworakowski, Thin Solid Films 393 (2001) 168.
[7] X.-H. Zhang, R. West, J. Polym. Sci. Polym. Chem. Ed. 22 (1984) 159.
[8] C.I. Aitken, J.F. Harrod, E. Samuel, J. Am. Chem. Soc. 108 (1986) 4059.
[9] Y. Hsiao, R.M. Waymouth, J. Am. Chem. Soc. 116 (1994) 9779.
[10] I. Kmínek, E. Brynda, W. Schnabel, Eur. Polym. J. 27 (1991) 1073.
[11] S. Nešpůrek, P. Toman, J. Sworakowski, Thin Solid Films, in press.
[12] S. Nešpůrek, H. Valerián, A. Eckardt, V. Herden, W. Schnabel, Polym. Adv. Technol. 12 (2001) 306.
[13] S. Nešpůrek, K. Ulbert, Cs. Cas. Fyz. 25A (1975) 144.
[14] S. Nešpůrek, A. Eckhardt, Polym. Adv. Technol. 12 (2001) 427.
[15] A. Eckhardt, S. Nešpůrek, W. Schnabel, Ber. Bunsenges. Phys. Chem. 98 (1994) 1325.
[16] A. Kadashchuk, N. Ostapenko, V. Zaika, S. Nešpůrek, Chem. Phys. 234 (1998) 285.
[17] F.C. Grozena, L.D.A. Siebbeles, J.M. Warman, S. Seki, S. Tagawa, U. Scherf, Adv. Mater. 14 (2002) 228.
[18] S. Nešpůrek, V. Herden, M. Kunst, W. Schnabel, Synth. Met. 109 (2000) 309.
[19] C.G. Pitt, R.N. Carey, E.C. Toren, Jr., J. Am. Chem. Soc. 94 (1972) 3806.
[20] D.W. Turner, C. Baker, A.D. Baker, C.R. Brundle, Molecular Photoelectron Spectroscopy, Wiley/Interscience, London, 1970.
[21] H. Bock, W. Ensslin, Angew. Chem. Int. Ed. Engl. 10 (1971) 404.
[22] R. West, in: Proceedings of the Symposium on Organosilicon, Pittsburgh, 1971.
[23] H. Frey, M. Möller, M.P. de Haas, N.J.P. Zenden, P.G. Schouten, G.P. van der Laan, J.M. Warman, Macromolecules 26 (1993) 89.
[24] J.W. Mintmire, Phys. Rev. B 39 (1989) 13350.
[25] Y.R. Kim, M. Lee, J.R.G. Thorne, R.M. Hochstrasser, J.M. Zeigler, Chem. Phys. Lett. 145 (1988) 75.
[26] J. Sworakowski, G.F. Leal Ferreira, J. Phys. D 17 (1984) 135.
[27] J. Sworakowski, M. Samoc, IEEE Trans. Elect. Insul. 22 (1987) 13.
[28] V.I. Arhipov, E.V. Emelianova, A. Kadashchuk, I. Blonsky, S. Nešpůrek, D.S. Weiss, H. Bässler, Phys. Rev. B 65 (2002) 165218.
[29] H. Bässler, P.M. Borsenberger, R.J. Perry, J. Polym. Sci. B 32 (1994) 1677.
[30] M. Abkowitz, M. Stolka, J. Inorg. Organomet. Polym. 1 (1991) 487.
[31] I.I. Fishchuk, A. Kadashchuk, H. Bässler, S. Nešpurek, Phys. Rev. B67 (2003) 224–303.
[32] L. Pan, M. Zhang, Y. Nakayama, J. Chem. Phys. 110 (1999) 10509.
[33] H. Valerián, E. Brynda, S. Nešpůrek, W. Schnabel, J. Appl. Phys. 78 (1995) 6071.
[34] S. Nešpůrek, J. Pfleger, E. Brynda, I. Kmínek, A. Kadashchuk, A. Vakhnin, J. Sworakowski, Mol. Cryst. Liq. Cryst. 355 (2001) 191.
[35] S. Nešpůrek, J. Sworakowski, A. Kadashchuk, IEEE Trans. Dielect. Elect. Insul. 8 (2001) 432.
[36] J. Sworakowski, S. Nešpůrek, in: A. Graja, B.R. Bulka, F. Kajzar (Eds.), Molecular Low Dimensional and Nanostructured Materials for Advanced Applications, Kluwer Academic Publishers, Dordrecht, 2002.
[37] J. Sworakowski, S. Nešpůrek, Polym. J. Chem. 72 (1998) 163.
[38] J. Sworakowski, IEEE Trans. Dielect. Elect. Insul. 7 (2000) 531.
[39] K. Navrátil, J. Šik, J. Humlícek, S. Nešpůrek, Opt. Mater. 12 (1999) 105.
[40] L.A. Harrah, J.M. Zeigler, Macromolecules 20 (1987) 610.
[41] K. Takeda, M. Fujino, K. Seki, J. Inokuchi, Phys. Rev. B 36 (1987) 8129.
[42] J.W. Mintmire, J.V. Ortiz, Macromolecules 21 (1988) 1189.
[43] K. Takeda, H. Teramae, N. Matsumoto, J. Am. Chem. Soc. 108 (1986) 8186.
[44] R.G. Kepler, Z.G. Soos, Phys. Rev. B 43 (1991) 12530.
[45] S. Nešpůrek, A. Kadashchuk, Yu. Skryshevski, A. Fujii, K. Yoshino, J. Luminescence 99 (2002) 131.
[46] H. Sakurai, H. Sugiyama, M. Kira, J. Phys. Chem. 94 (1990) 1837.
[47] F. Schauer, R. Handlír, S. Nešpůrek, Adv. Mater. Opt. Elect. 7 (1997) 61.
[48] R.G. Kepler, J.M. Zeigler, L.A. Harrah, S.R. Kurtz, Phys. Rev. B 35 (1982) 2819.
[49] V. Cimrová, S. Nešpůrek, Synth. Met. 64 (1994) 271.
[50] S. Nešpůrek, V. Cimrová, Prog. Colloid. Polym. Sci. 78 (1988) 88.
[51] S. Nešpůrek, V. Cimrová, J. Pfleger, I. Kmínek, Polym. Adv. Technol. 7 (1996) 459.
[52] R.G. Kepler, J.M. Ziegler, Mater. Res. Soc. Proc. 173 (1990) 453.
[53] V. Cimrová, S. Nešpůrek, R. Kuzel, W. Schnabel, Synth. Met. 67 (1994) 103.
[54] S. Irie, M. Irie, Macromolecules 25 (1992) 1766.
[55] S. Irie, H. Horri, M. Irie, Macromolecules 13 (1980) 1355.
[56] Y. Ohsako, J.R.G. Thorne, C.M. Phillips, J.M. Zeigler, R.M. Hochstrasser, J. Phys. Chem. 93 (1989) 4408.
[57] T. Karatsu, R.D. Miller, R. Sooriyakumaran, J. Michl, J. Am. Chem. Soc. 111 (1989) 1140.
[58] B. Cercek, M. Kongshang, J. Phys. Chem. 74 (1970) 4319.
[59] H. Dürr, H. Bouas-Laurent (Eds.), Photochromism, Molecules and Systems, Elsevier, Amsterdam, 1990.
[60] J. Sworakowski, Mol. Cryst. Liq. Cryst. 11 (1970) 1.